NUCL SCI TECH (2020) 31:49
https://doi.org/10.1007/s41365-020-00758-x

Energy calibration of HPGe detector using the high-energy characteristic γ rays in ^{13}C formed in ^{6}Li + ^{12}C reaction

Jia-Tai Li[1,2] · Xue-Dou Su[1] · Gao-Long Zhang[1,3] · Guang-Xin Zhang[4,5] · Shi-Peng Hu[6] · Jing-Bin Lu[7] · Yi-Feng Lv[7] · Hui-Bin Sun[6] · Huan-Qiao Zhang[8] · D. Testov[4,5] · P. R. John[4,5] · J. J. Valiente-Dobón[9] · A. Goasduff[4,5] · M. Siciliano[9,10] · F. Galtarossa[9] · F. Recchia[4,5] · D. Mengoni[4,5] · D. Bazzacco[4,5]

Received: 11 October 2019 / Revised: 23 February 2020 / Accepted: 25 February 2020 / Published online: 4 May 2020

Abstract An ^{6}Li + ^{89}Y experiment was conducted at the Laboratori Nazinali di Legnaro, INFN, Italy. The 550 μg/cm^2 thick ^{89}Y target was backed on a 340 μg/cm^2 thick ^{12}C foil. The several γ rays in the experiment with energies higher than 3000 keV can most likely be ascribed to the transitions in the ^{13}C nuclei, which can be formed through various interactions between the ^{6}Li beam and the ^{12}C foil. The high-energy properties of γ rays in ^{13}C are employed for energy calibrating HPGe detectors, especially for the >3000 keV region, which is impossible to reach by common standard sources (^{152}Eu, ^{133}Ba, etc.). Furthermore, γ–γ and particle–γ coincidence measurements were performed to investigate the formation of ^{13}C.

Keywords Energy calibration · Coincidence measurement · Weakly bound nuclei · Reaction mechanism

1 Introduction

Owing to their excellent energy resolution, high-purity germanium (HPGe) detectors are widely employed in the detection of γ transitions. In γ-ray spectroscopy experiments, the energy calibration of HPGe detectors is critical. To perform a reliable energy calibration for HPGe detectors, a set of standard radioactive sources that can emit many γ rays with precisely known energies are used, such as ^{152}Eu, ^{133}Ba, ^{60}Co, and ^{137}Cs. However, when the high-energy γ rays (for instance, $E_\gamma > 3500\,\mathrm{keV}$) require analysis, such energy regions cannot be calibrated by the aforementioned sources since none of them can produce the required intense γ rays with energies higher than 3500 keV [1, 2]. Moreover, the few standard radioactive sources that can emit γ rays with energies higher than 1500 keV have short lifetimes [3]: ^{66}Ga

This work was supported by the National Natural Science Foundation of China (Nos. 11975040, U1832130, 11475013) and the HIRFL User Project, CAS.

✉ Gao-Long Zhang
zgl@buaa.edu.cn

Guang-Xin Zhang
Guangxin.Zhang@pd.infn.it

1 School of Physics, Beihang University, Beijing 100191, China

2 Shenyuan Honors College, Beihang University, Beijing 100191, China

3 Beijing Advanced Innovation Center for Big Data-Based Precision Medicine, School of Medicine and Engineering, Beihang University and Key Laboratory of Big Data-Based Precision Medicine (Beihang University), Ministry of Industry and Information Technology, Beihang University, Beijing 100191, China

4 Dipartimento di Fisica Astronomia, dell'Universit'a di Padova, Padua, Italy

5 Istituto Nazionale di Fisica Nucleare, Sezione di Padova, Padua, Italy

6 College of Physics Science and Technology, Shenzhen University, Shenzhen 518060, China

7 College of Physics, Jilin University, ChangChun 130012, China

8 China Institute of Atomic Energy, Beijing 102413, China

9 Laboratori Nazionali di Legnaro, INFN, Legnaro, Padua, Italy

10 Irfu/CEA, Universit de Paris-Saclay, Gif-sur-Yvette, France

(833.5–4806 eV, 13 γ rays in total, $T_{1/2}$ = 9.49 h), 10 γ rays have energies higher than 1500 keV; ^{24}Na (1368.6 and 2754 keV, $T_{1/2}$ = 14.997 h); ^{56}Co (846.8–3548.1 keV, 14 γ rays in total, $T_{1/2}$ = 77.236 d), 9 γ rays have energies higher than 1500 keV [2, 3].

Assuming that one HPGe detector is calibrated by the ^{152}Eu source, this detector could exclusively measure γ rays with energies up to approximately 1500 keV since the measured energy is only valid in that calibration region. In the extrapolation region, the measured energy derived from the calibration coefficient might deviate significantly from the real value. The situation would be improved if any known high-energy γ rays, produced either by the radioactive source [3] or the in-beam experiment, could be employed in the energy calibration procedure.

The investigation of reaction mechanisms induced by stable weakly bound nuclei (such as ^{6,7}Li) has drawn considerable attention during the last few decades [4–18]. Owing to the low breakup threshold and the strong cluster structure of the weakly bound nuclei, ^{7}Li has an $\alpha + t$ cluster structure and a small separation energy of 2.47 MeV. Also the breakup, as well as the transfer channels, may couple to the fusion reaction especially when the beam energies approach the Coulomb barrier, leading to a series of complicated and interesting processes [5, 10, 19–35].

In a fusion reaction study [10, 30, 33], γ-ray spectroscopy has already proven to be powerful since, in principle, the yields of each residual nucleus (excited states) can be obtained by counting their characteristic γ transitions. For this study, a ^{6}Li + ^{89}Y experiment was performed in the Laboratori Nazinali di Legnaro (LNL), INFN, Italy. In this experiment, the ^{89}Y's target back material was ^{12}C foil. Details of the experimental procedure are recorded in Sect. 2. Several possible reaction processes between the ^{6}Li beam and the ^{12}C foil produce ^{13}C nuclei as by-product. Nevertheless, as discussed in Sect. 3, the characteristic γ rays (3684.5 and 3853.8 keV) in ^{13}C were applied to calibrate the HPGe detector. Furthermore, in the same section, the presence of ^{13}C was confirmed by γ–γ analysis and the possible reaction mechanisms that may be responsible for the production of ^{13}C were investigated by particle–γ coincidence analysis. It should be noted that such energy calibration methods might be appropriate for other experiments when the targets are backed with a carbon foil.

2 Experimental procedure

This ^{6}Li + ^{89}Y experiment was conducted using the INFN-LNL Tandem-XTU accelerator in Italy. A ^{6}Li^{3+} beam with E_{Lab} = 34 MeV and an average beam intensity of 1.0 enA was impinged on a 550 μg/cm^2 thick ^{89}Y target, which was backed by 340 μg/cm^2 thick ^{12}C foil. A schematic view of the detector arrays obtained from [36] is shown in Fig. 1. Around the target position, 40 ΔE–E silicon detectors (a silicon-ball named EUCLIDES [37]) and 25 HPGe detectors (GALILEO array [37]) were used to measure the light-charged particles and γ rays, respectively. Each ΔE detector had a thickness of 130 μm, and the E detector had a thickness of 1 mm. The GALILEO array had 10 HPGe detectors at 90° relative to the beam direction, and another 15 detectors were equally spaced at 119°, 129°, 152° [38–40]. Along the beam direction, an Al cylindrical absorber with a thickness of 200 μm was inserted inside EUCLIDES to protect the silicon detectors from elastically scattered beams. Additional experimental details can be found in the previous publication [36].

3 Data analysis

3.1 Calibration of γ-ray energy spectrum

In the current experiment, the HPGe detectors were initially calibrated by the standard radioactive sources including ^{60}Co, ^{88}Y, ^{133}Ba and ^{152}Eu, and the function of

$$E_{\mathrm{standard}} = \sum_{j=0}^{5} b_j \times \mathrm{Channel}^j \quad (1)$$

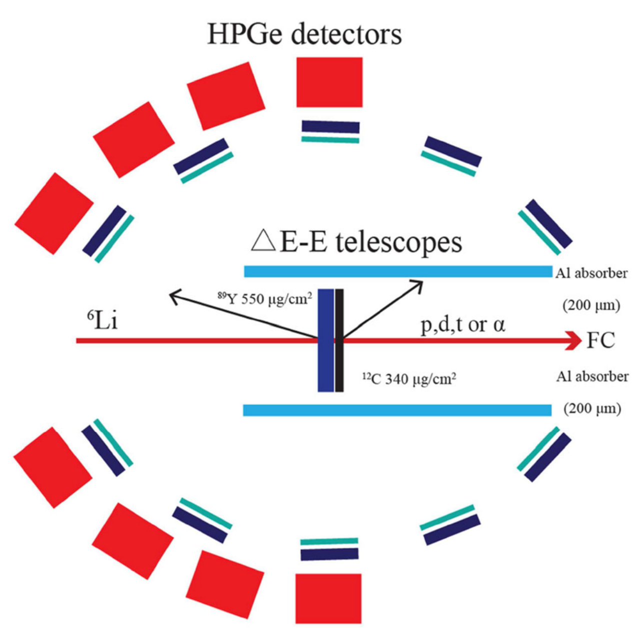

Fig. 1 (Color online) Schematic view of detector array around the target position, which is obtained from [36]; 40 ΔE–E silicon telescopes and 25 HPGe detectors are used to measure the light-charged particles and γ rays, respectively

was used to perform the first energy calibration step. Here, E_{standard} represents the energy of known γ rays emitted from the aforementioned sources, Channel is the channel position of each γ ray in the raw ADC (specific name of ADC in front and ADC in the bracket) spectrum, and b_j relates to the calibration coefficients. It is noted here that in the current stage, the highest $E_{\text{standard}} = 2734$ keV (^{88}Y source). Thus, in the experiment, a measured γ ray with energy higher than 2800 keV may be observed in a position different from its actual energy, and such deviations can vary between different detectors.

The partial level scheme and several known γ rays in ^{13}C are displayed in Table 1 and Fig. 2, respectively [2, 41]. After the first-step calibration, Fig. 3a shows the γ-ray energy spectrum measured by different HPGe detectors at 90° during the $^{6}\text{Li} + {}^{89}\text{Y}$ experiment. It was observed that the peak positions varied among different detectors.

Since the first-step energy calibration included the E_{standard} up to 2734 keV, the γ-ray energies measured in the region shown in Fig. 3a could be inaccurate. Conversely, detectors at 90° in Fig. 3a were selected to avoid a possible Doppler shift effect on the γ-ray measurement. In conclusion, the incorrect calibration in this energy region becomes the only possible explanation for the phenomenon shown in Fig. 3a. The two γ rays observed in each detector in Fig. 3a are probably attributed to the 3684.5 and 3853.8 keV transitions de-exciting the 3853.8 keV state in ^{13}C as shown in Fig. 2. Further confirmation of this assumption can be found in the following two subsections.

A second-step calibration of the HPGe detector could then be performed. The γ rays which were used in the previous calibration, as well as 3684.5- and 3853.8-keV γ rays in ^{13}C were employed in the new energy calibration for the same functions Eq. 1 as shown before. The newly calibrated γ-ray energy spectra of each HPGe detector at 90° are shown in Fig. 3b which are shown in the same energy region by Fig. 3a. It can be concluded that the second-step energy calibration solves the energy discrepancy for the γ rays with $E_\gamma > 3500\,\text{keV}$ in Fig. 3b. The newly calibrated γ-ray energy spectra having different

Table 1 Partial characteristic γ transitions in ^{13}C with $E_\gamma < 4000\,\text{keV}$ [2, 41]

E_γ(keV)	Transitions
169.3	$5/2^+ \xrightarrow{E1} 3/2^-$
595.1	$3/2^- \xrightarrow{E1} 1/2^+$
764.4	$5/2^+ \xrightarrow{E2} 1/2^+$
3089.4	$1/2^+ \xrightarrow{E1} 1/2^-$
3684.5	$3/2^- \xrightarrow{M1+E2} 1/2^-$
3853.8	$5/2^+ \xrightarrow{M2+E3} 1/2^-$

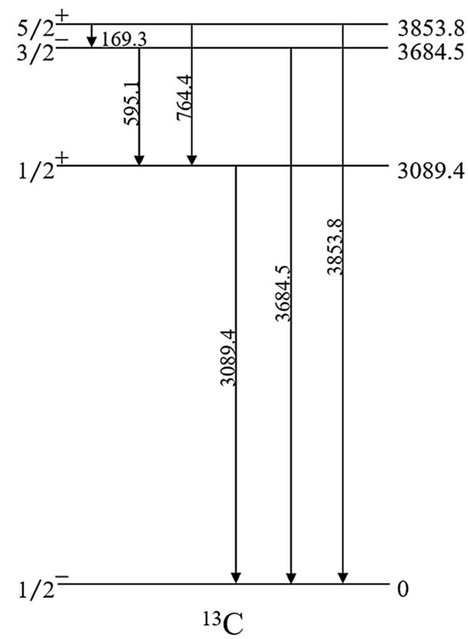

Fig. 2 Partial level scheme of ^{13}C below the excitation energy of 4000 keV. The unit of energy for each state and the γ transition is keV [2, 41]

energy regions are also shown in Fig. 4. It can be seen in Fig. 4 that besides the γ transitions in ^{13}C, other peaks corresponding to fusion-evaporation residues, such as ^{92}Mo, produced from the $^{6}\text{Li} + {}^{89}\text{Y}$ system were identified.

3.2 γ–γ coincidence analysis

In this section, γ–γ coincidence analysis, which is based on the result of the aforementioned second calibration, is applied to confirm the partial level scheme of ^{13}C as shown in Fig. 2.

Figure 5a–c shows the γ-ray spectra which were gated by the 169.3-, 764.4- and 3089.4-keV transitions, respectively. From Fig. 5a, b, it can be concluded that the 169.3- and 3684.5-keV γ rays were in coincidence with each other, and the 764.4- and 3089.4-keV γ rays were also in coincidence with each other. Figure 5c not only re-confirms the coincidence between the 764.4- and 3089.4-keV transitions but also establishes the cascade order by identifying the 595.1-keV γ rays which were mutually in coincidence with the 169.3- and 3089.4-keV transitions. Consequently, this experiment confirmed the partial level scheme as shown in Fig. 2.

Because the γ transitions with energies higher than 3000-keV are frequently referenced in previous explications, it may be concluded that without the second calibration, the level scheme confirmation of ^{13}C cannot be performed. The success in reconstructing the ^{13}C level

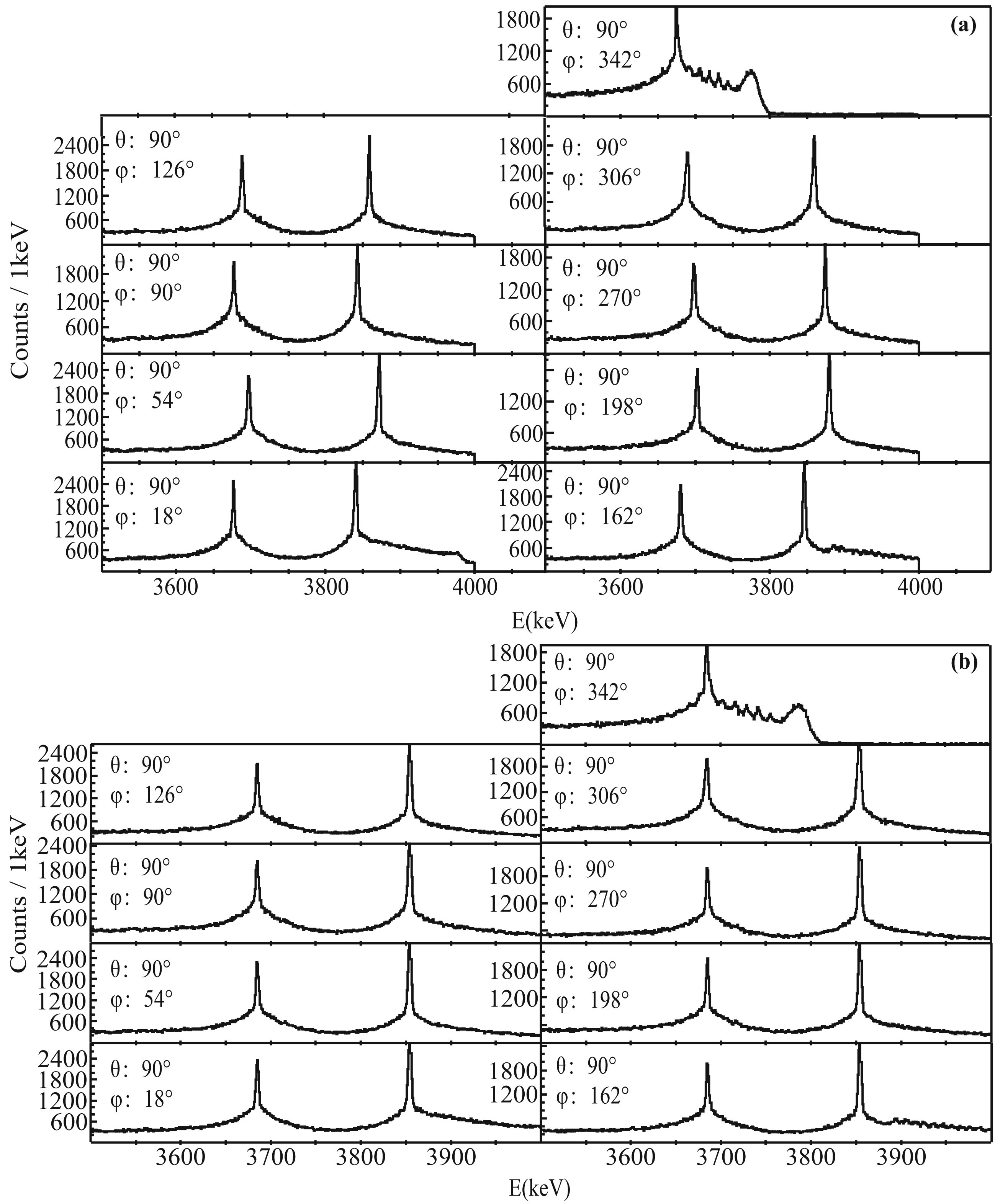

Fig. 3 γ-Ray energy spectrum of 10 HPGe detectors at 90° (3500 keV < E_γ < 4000 keV). **a** The first-step calibration, **b** the second-step calibration

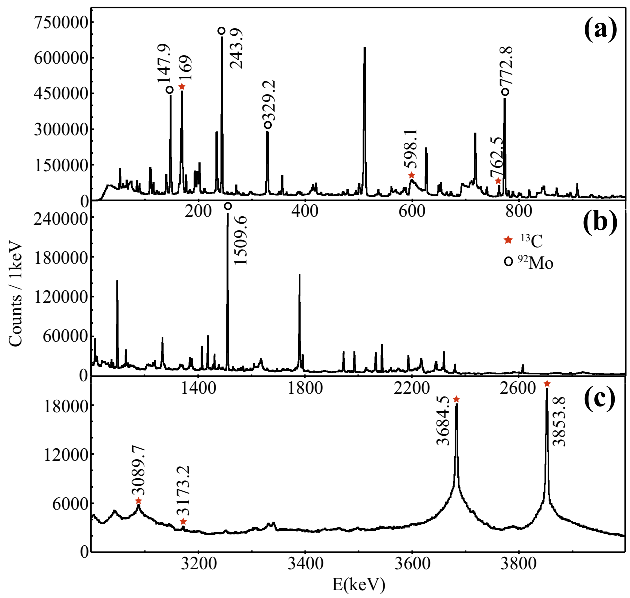

Fig. 4 Newly calibrated γ-ray energy spectra. **a** $E_\gamma < 1000$ keV, **b** $1000\text{ keV} < E_\gamma < 2000$ keV, **c** $3000\text{ keV} < E_\gamma < 4000$ keV

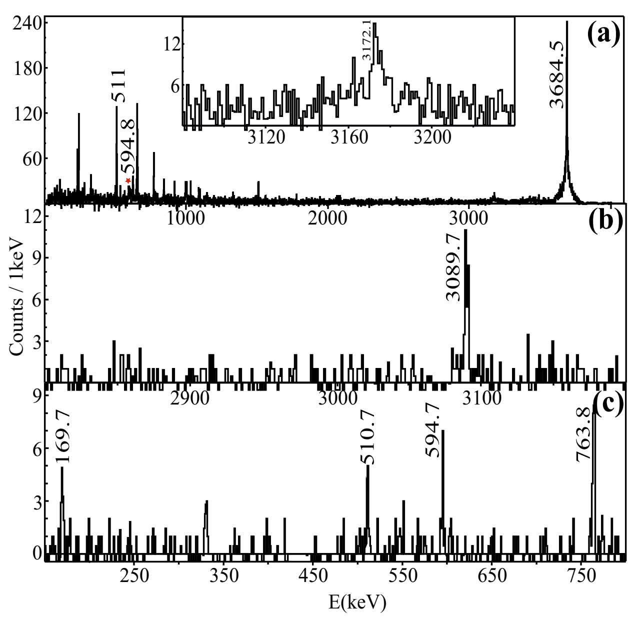

Fig. 5 γ-Ray energy spectra gated by the **a**169.3-keV γ ray, **b** the 764.4-keV γ ray and **c** the 3089.4-keV γ ray

scheme proves reasonable the assumption that the γ rays observed in Fig. 3 belong to ^{13}C.

Moreover, 511 and 3172.1 keV γ rays can be identified in the newly calibrated γ-ray energy spectra and γ-ray energy spectrum which is gated by the 169.3-keV γ ray (see Fig. 5a). Since 3172.1-keV is approximately 511 keV smaller than 3684.5-keV, it is concluded that the 3172.1-keV peak is the single escape peak of the 3684.5-keV γ ray.

3.3 Particle–γ coincidence analysis

Figure 6a, b displays the γ-ray energy spectra which are measured in coincidence with protons and α particles, respectively. The characteristic γ rays of ^{13}C at 168.8-, 598.6-, 762.5-, 3684.6- and 3853.8-keV (see Table 1) are clearly visible in Fig. 6a. The characteristic γ rays of ^{13}C at 168.7- and 598.2-keV can also be observed in Fig. 6b with low statistics. The other characteristic γ rays of ^{13}C as listed in Table 1 cannot be seen in Fig. 6b owing to their low relative intensities [2]. Thus, it can be concluded that (at least part of) the ^{13}C nuclei are created in coincidence with α and protons.

Considering the possible reaction channels, there are several possible causal processes, such as (1) one-neutron stripping process, denoted as $^{6}\text{Li} + {}^{12}\text{C} \longrightarrow {}^{5}\text{Li} + {}^{13}\text{C}^*$ (there is no bound state for ^{5}Li, and thus, it will disassociate into a proton and α immediately), (2) complete fusion of $^6\text{Li} + {}^{12}\text{C}$ followed by the $1\alpha1p$ evaporation channel, and (3) an incomplete fusion channel. This means that the ^{6}Li breaks up to α and deuteron, and the deuteron is then captured by the ^{12}C, followed by one-proton evaporation. All the aforementioned processes might account for the production of the ^{13}C nuclei, since such (1)–(3) channels can populate ^{13}C with excited states, as well as α and proton particles, being consistent with the experimental observations. A more detailed, or quantitative investigation of the causal processes requires additional measurement of the charged particles (α and protons) with considerably higher energy resolution.

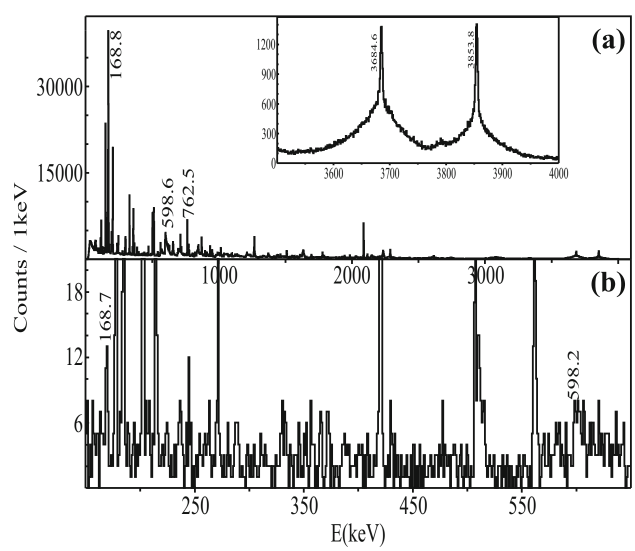

Fig. 6 The γ-ray energy spectra, which are measured in coincidence with **a** protons and **b** α particles, respectively

4 Summary

A ^{6}Li + ^{89}Y experiment to study fusion reactions induced by weakly bound nuclei was performed at INFN-LNL in Italy. ^{13}C can be formed by the one-neutron stripping process, complete fusion channel and incomplete fusion channel between the ^{6}Li beam, and the ^{12}C back material. The characteristic γ rays of ^{13}C can be used for energy calibrating HPGe detectors in the high-energy region. It is concluded that this method is appropriate for other experiments with carbon foil and can contribute to the investigation of high-energy γ rays. The partial level scheme of ^{13}C is confirmed by γ–γ coincidence analysis, and the formation of ^{13}C in the ^{6}Li + ^{12}C system was investigated by particle–γ coincidence analysis.

Acknowledgements We are grateful to the INFN-LNL staff for providing a stable ^{6}Li beam throughout the experiment.

References

1. E.K. Warburton, D.E. Alburger, D.J. Millener, Energies and branching ratios of transitions in ^{13} C . Phys. Rev. C **22**(6), 2330–2340 (1980). https://doi.org/10.1103/PhysRevC.22.2330
2. F. Ajzenberg-selove, J.H. Kelley, C.D. Nesaraja. Adopted levels, gammas for ^{13}C. www.nndc.bnl.gov. Accessed 1 Oct 2019
3. Z.R. Shi, K. Xu, L.H. Li, *Standard Source of High Energy γ-Ray* (China Institute of Atomic Energy, Beijing, 2008), pp. 206–210. **(in Chinese)**
4. L.F. Canto, P.R.S. Gomes, R. Donangelo, M.S. Hussein, fusion and breakup of weakly bound nuclei. Phys. Rep. **424**(1–2), 1–111 (2006). https://doi.org/10.1016/j.physrep.2005.10.006
5. L.F. Canto, P.R.S. Gomes, R. Donangelo et al., Recent developments in fusion and direct reactions with weakly bound nuclei. Phys. Rep. **596**, 1–86 (2015). https://doi.org/10.1016/j.physrep.2015.08.001
6. J. Lei, A.M. Moro, Puzzle of complete fusion suppression in weakly bound nuclei: a trojan horse effect? Phys. Rev. Lett. **122**, 042503 (2019). https://doi.org/10.1103/PhysRevLett.122.042503
7. J. Lei, A.M. Moro, Unraveling the reaction mechanisms leading to partial fusion of weakly bound nuclei. Phys. Rev. Lett. **123**, 232501 (2019). https://doi.org/10.1103/PhysRevLett.123.232501
8. B.B. Back, H. Esbensen, C.L. Jiang et al., Recent developments in heavy-ion fusion reactions. Rev. Mod. Phys. **86**, 317–360 (2014). https://doi.org/10.1103/RevModPhys.86.317
9. C. Beck, N. Rowley, P. Papka et al., Reaction mechanisms for weakly-bound, stable nuclei and unstable, halo nuclei on medium-mass targets. Nucl. Phys. A **834**(1–4), 440c–445c (2010). https://doi.org/10.1016/j.nuclphysa.2010.01.059
10. S.P. Hu, G.L. Zhang, J.C. Yang et al., Small suppression of the complete fusion of the ^{6}Li + ^{96}Zr system at near-barrier energies. Phys. Rev. C **91**, 044619 (2015). https://doi.org/10.1103/PhysRevC.91.044619
11. C.L. Guo, G.L. Zhang, S.P. Hu et al., Coupling effects on the fusion of ^{6}Li + ^{154}Sm at energies slightly above the Coulomb barrier. Phys. Rev. C **92**, 014615 (2015). https://doi.org/10.1103/PhysRevC.92.014615
12. M.F. Guo, G.L. Zhang, P.R.S. Gomes et al., Negligible suppression of the complete fusion of 6,7Li on light targets, at energies above the barrier. Phys. Rev. C **94**, 044605 (2016). https://doi.org/10.1103/PhysRevC.94.044605
13. M. Mazzocco, N. Keeley, A. Boiano et al., Elastic scattering for the ^{8}B and ^{7}Be + ^{208}Pb systems at near-Coulomb barrier energies. Phys. Rev. C **100**, 024602 (2019). https://doi.org/10.1103/PhysRevC.100.024602
14. G.L. Zhang, G.X. Zhang, C.J. Lin et al., Angular distribution of elastic scattering induced by ^{17}F on medium-mass target nuclei at energies near the Coulomb barrier. Phys. Rev. C **97**, 044618 (2018). https://doi.org/10.1103/PhysRevC.97.044618
15. G.L. Zhang, X.P. Yang, H.Q. Zhang, Systematic study on reaction function of weakly bound nuclei. Nucl. Sci. Tech. **37**(10), 100508 (2014). https://doi.org/10.11889/j.0253-3219.2014.hjs.37.100508 (in Chinese)
16. L. Yang, C.J. Lin, H.M. Jia et al., Is the dispersion relation applicable for exotic nuclear systems? The abnormal threshold anomaly in the 6He + 209Bi system. Phys. Rev. Lett. **119**, 042503 (2017). https://doi.org/10.1103/PhysRevLett.119.042503
17. A. Di Pietro, G. Randisi, V. Scuderi et al., Elastic scattering and reaction mechanisms of the halo nucleus ^{11}Be around the Coulomb barrier. Phys. Rev. Lett. **105**, 022701 (2010). https://doi.org/10.1103/PhysRevLett.105.022701
18. E.F. Aguilera, P. Amador-Valenzuela, E. Martinez-Quiroz et al., Near-barrier fusion of the ^{8}B + ^{58}Ni proton-halo system. Phys. Rev. Lett. **107**, 092701 (2011). https://doi.org/10.1103/PhysRevLett.107.092701
19. R. Raabe, J.L. Sida, J.L. Charvet et al., No enhancement of fusion probability by the neutron halo of ^{6}He. Nature **431**, 823–826 (2004). https://doi.org/10.1038/nature02984
20. A. Di Pietro, P. Figuera, F. Amorini et al., Reactions induced by the halo nucleus ^{6}He at energies around the Coulomb barrier. Phys. Rev. C **69**, 044613 (2004). https://doi.org/10.1103/PhysRevC.69.044613
21. L. Acosta, A.M. Sanchez-Benitez, M.E. Gomez et al., Elastic scattering and α-particle production in ^{6}He + ^{208}Pb collisions at 22 MeV. Phys. Rev. C **84**, 044604 (2011). https://doi.org/10.1103/PhysRevC.84.044604
22. E.F. Aguilera, J.J. Kolata, F.M. Nunes et al., Transfer and/or breakup modes in the ^{6}He + ^{209}Bi reaction near the Coulomb barrier. Phys. Rev. Lett. **84**, 5058 (2000). https://doi.org/10.1103/PhysRevLett.84.5058
23. A. Navin, V. Tripathi, Y. Blumenfeld et al., Direct and compound reactions induced by unstable helium beams near the Coulomb barrier. Phys. Rev. C **70**, 044601 (2004). https://doi.org/10.1103/PhysRevC.70.044601
24. A. Lemasson, A. Navin, N. Keeley et al., Reactions with the double-Borromean nucleus ^{8}He. Phys. Rev. C **82**, 044617 (2010). https://doi.org/10.1103/PhysRevC.82.044617
25. A. Chatterjee, A. Navin, A. Shrivastava et al., 1n and 2n transfer with the Borromean nucleus ^{6}He near the Coulomb barrier. Phys. Rev. Lett. **101**, 032701 (2008). https://doi.org/10.1103/PhysRevLett.101.032701
26. C. Signorini, A. Edifizi, M. Mazzocco et al., Exclusive breakup of ^{6}Li by ^{208}Pb at Coulomb barrier energies. Phys. Rev. C **67**, 044607 (2003). https://doi.org/10.1103/PhysRevC.67.044607
27. K.J. Cook, E.C. Simpson, L.T. Bezzina et al., Origins of incomplete fusion products and the suppression of complete fusion in reactions of ^{7}Li. Phys. Rev. Lett. **122**, 102501 (2019). https://doi.org/10.1103/PhysRevLett.122.102501
28. A. Shrivastava, A. Navin, A. Diaz-Torres et al., Role of the cluster structure of ^{7}Li in the dynamics of fragment capture. Phys. Lett. B **718**, 931–936 (2013). https://doi.org/10.1016/j.physletb.2012.11.064
29. A. Shrivastava, A. Navin, A. Lemasson et al., Exploring fusion at extreme sub-barrier energies with weakly bound nuclei. Phys.

Rev. Lett. **103**, 232702 (2009). https://doi.org/10.1103/PhysRevLett.103.232702

30. S.P. Hu, G.L. Zhang, J.C. Yang et al., One-neutron stripping process to excited states of the ^{6}Li + ^{96}Zr reaction at near-barrier energies. Phys. Rev. C **93**(1), 014621 (2016). https://doi.org/10.1103/PhysRevC.93.014621
31. C.S. Palshetkar, S. Thakur, V. Nanal et al., Fusion and quasi-elastic scattering in the ^{6,7}Li + ^{197}Au systems. Phys. Rev. C **89**(2), 024607 (2014). https://doi.org/10.1103/PhysRevC.89.024607
32. M.F. Werby, S. Edwards, Study of neutron and alpha-particle transfer mechanisms in the ^{7}Li(d, t)^{6}Li reaction. Phys. Rev. C **8**(3), 978–987 (1973). https://doi.org/10.1103/PhysRevC.8.978
33. G.L. Zhang, G.X. Zhang, S.P. Hu et al., One-neutron stripping processes to excited states of ^{90}Y* in the ^{89}Y(^{6}Li,^{5}Li)^{90}Y* reaction. Phys. Rev. C **97**, 014611 (2018). https://doi.org/10.1103/PhysRevC.97.014611
34. W.J. Li, Y.G. Ma, G.Q. Zhang et al., Yield ratio of neutrons to protons in ^{12}C (d,n)^{13}N and ^{12}C (d,p)^{13}C from 0.6 to 3 MeV. Nucl. Sci. Tech. **30**, 180 (2019). https://doi.org/10.1007/s41365-019-0705-0
35. W. Liu, J.L. Lou, Y.L. Ye et al., Experimental study of intruder components in light neutron-rich nuclei via single-nucleon transfer reaction. Nucl. Sci. Tech. **31**, 20 (2020). https://doi.org/10.1007/s41365-020-0731-y
36. S.P. Hu, G.L. Zhang, G.X. Zhang et al., A powerful combination measurement for exploring the fusion reaction mechanisms induced by weakly bound nuclei. Nuclear Instrum. Methods Phys. Res. A **914**(11), 64–68 (2019). https://doi.org/10.1016/j.nima.2018.05.067
37. D. Testov, D. Mengoni, A. Goasduff et al., The 4π highly-efficient light-charged-particle detector EUCLIDES, installed at the GALILEO array for in-beam γ-ray spectroscopy. Eur. Phys. J. A **55**(4), 47 (2019). https://doi.org/10.1140/epja/i2019-12714-6
38. J. J. Valiente-Dobón, D. Mengoni, F. Recchia, et al. INFN-LNL Annual Report No. 95, 2014
39. D. Testov, D. Mengoni, C. Boiano, et al., The first physical campaign of the EUCLIDES Si-ball detector coupled to GALILEO gamma-ray spectrometer. INFN-LNL Annual Report No. 105, 2015
40. A. Gadea, E. Farnea, G. de Angelis, et al., A new Charged particle Si detector for EUROBALL. INFN-LNL Annual Report No. 225, 1996
41. F. Ajzenberg-Selove, Energy levels of light nuclei A = 13–15. Nucl. Phys. A **268**(1), 1–204 (1976). https://doi.org/10.1016/0375-9474(76)90563-7